Alternative Method to Determine a Carbon Dioxide Removal Target

Shannon A. Fiume
Open NanoCarbon, San Francisco, CA USA
Correspondence: shannon@autofracture.com

Abstract

We show how to determine the amount of carbon to remove to affect the cumulative emitted anthropogenic carbon dioxide in order to create Carbon Dioxide Removal (CDR) targets, additionally, compare anthropogenic carbon dioxide emissions growth to the late Holocene carbon dioxide atmospheric concentration for historical context and present hypothetical emissions declines for climate restoration. We explore the historical context of cumulative anthropogenic carbon dioxide emissions and how it's induced increases to each of the natural sinks. To obtain more comprehensive CDR targets, we present a new method to calculate the total amount of carbon to remove from cumulative CO_2 emissions that are present in natural sinks. Determining total emissions removed is obscured when only considering yearly emissions change. A possible baseline CO_2 concentration of 280.9 ± 0.9 ppm for pre-human change stretching from 600 BCE to 1750 CE, was found and could be explored separately. We show multiple speculative emission declines to zero cumulative CO_2 emissions to reach complete climate restoration. For groups seeking climate restoration which completes in less than half a human lifespan, a pair of emission declines is presented which complete in twenty years. The declines bound complete climate restoration in the shortest time and the more typical end of the century, 2100 target. There is a tradeoff between how fast the climate can be restored compared to how long humans can continue to emit carbon dioxide from the use of fossil fuels and land use change. We conclude with climate reversibility for maximum bounded idealized likely shortest hypotheses declines.

1. Introduction

As the Earth is a closed system, anthropogenic CO_2 emissions move to reside in natural sinks. Human activity from fossil fuel emissions and land-use change has radically increased the carbon composition of the Earth's natural sinks by exponential emissions increases since pre-industrial times.

The carbon dioxide between the atmosphere and oceans sinks are balanced by atmospheric chemistry: atmospheric CO_2 exerts pressure on CO_2 dissolved in the ocean surface waters (Takahashi et al., 2002). When CO_2 is removed from the atmosphere, the reduced CO_2 pressure allows the dissolved CO_2 remaining in the surface waters to outgas back to the atmosphere. Even though only about 50% of anthropogenic carbon stored in the ocean sink is in the top 400 meters (Sabine et al., 2004), the top 100 meters of surface waters contains the highly bioactive euphotic zone and is strongly negatively impacted by induced warming and acidification from anthropogenic carbon, additionally causing extensive damage to the marine ecology. Carbon dioxide dissolved in surface waters should be moved to more permanent storage, to stop affecting the surface waters or atmosphere.

The exponential forcing of cumulative emissions is often not considered and it's not readily apparent in the reporting of yearly changes in emissions. Even considering the uncertainty of ±5% at medium confidence level of the current estimated cumulative anthropogenic emissions of 432 gigatonnes carbon (GtC) per the Global Carbon Budget 2017 (Le Quéré et al., 2018), there is a large difference between achieving the Representative Concentration Pathway (RCP) 1.9 which could lower cumulative emissions under 200 GtC, and zero GtC. Additionally complicating removal efforts is how to determine the entire amount of carbon dioxide to remove. Without considering the carbon dioxide from all sinks, and the rebalancing that occurs when carbon dioxide is removed from a sink, only converting atmospheric carbon dioxide concentration in ppm for a removal target leads to drawing down only the atmospheric sink.

In order to more accurately estimate the amount of carbon dioxide to remove for Carbon Dioxide Removal (CDR) and ultimately climate restoration, we examine the total accumulation of carbon to the natural sinks from anthropogenic carbon dioxide emissions. We cover the differences between cumulative and yearly changes in emissions and highlight possible misinterpretation in solely examining yearly changes in emissions. We then provide estimates on possible carbon removal emission declines. This work does not prescribe how carbon dioxide can or should be removed from the atmosphere. Determining the appropriateness of a given CDR technology over another, or constructing a blend of technologies is beyond the scope of this work. This work exclusively focuses on the greenhouse gas carbon dioxide calculations for climate restoration and subsequently CDR, and does not cover other greenhouse gases.

2. Anthropogenic Emitted Carbon, What and Where?

The fossil fuel emissions from humans burning carbon-based fuels have over the years shifted between three major natural carbon sinks: land, ocean, and the atmosphere. Including the latest 2017 estimates, the total emitted carbon from anthropogenic CO_2 since 1750 is 627 GtC where 432 GtC is from fossil fuel emissions and 195 GtC from land-use change (Le Quéré et al., 2018). The atmosphere currently sinks about 271 GtC (Dlugokencky et al., 2018) in anthropogenic emissions. Emissions from human-induced land use change which roughly equals the land sink. The natural sinks contain more carbon than the introduced anthropogenic carbon. This work focuses on the increases to the total carbon in the natural sinks from anthropogenic emissions sources only. Carbon quantities are listed in gigatonnes carbon (GtC) or the equivalent petagrams carbon (PgC). To obtain gigatonnes CO_2, multiply by a conversion factor of 3.664 (Le Quéré et al., 2018).

Total Cumulative Anthropogenic Emissions	Fossil Fuel Emissions	Land-use Change Emissions	Land Sink	Ocean Sink	Atmospheric Sink*	Budget Imbalance
627.1	431.6	195.5	-189.8	-157.5	-271.3	-8.5

Table 1 | All values are from the Global Carbon Budget (Le Quéré et al., 2018) except the Atmospheric Sink. The atmospheric sink was generated from the current Global CO_2 Concentration from Mauna Loa (Dlugokencky et al., 2018) and converted to GtC via subtracting 277 ppm and multiplied by the conversion factor 2.12 (Ballantyne et al., 2012).

The year to year change in cumulative anthropogenic fossil fuel emissions results in strong exponential growth that is highly correlated to carbon growth in atmospheric, ocean and land sinks. Figure 1 plots the cumulative anthropogenic carbon from fossil fuels and land-use change CO_2 emissions per year, and how that carbon dioxide is distributed to the natural sinks. To complete the atmospheric dataset the Keeling Curve is shown in light blue overlaying the cumulative atmospheric yearly growth from the Global Carbon Budget 2017 (Le Quéré et al., 2018). The Keeling Curve is the globally averaged CO_2 concentration measured at Mauna Loa from 1980 to 2017

(Dlugokencky et al., 2018) was converted to GtC by the conversion factor of 2.12 (Ballantyne et al., 2012). Natural sink curves also show slower growing exponential curves. The steepest part of the cumulative fossil fuel emissions curve happened within the last two decades.

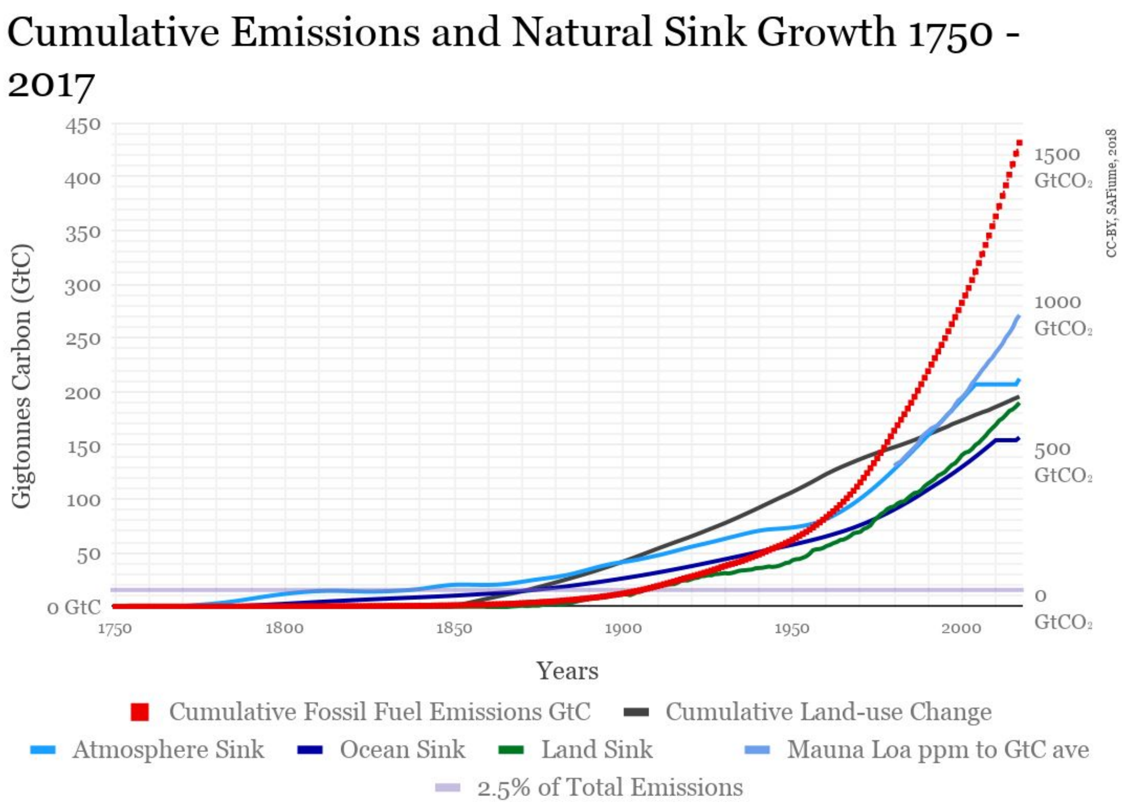

Figure 1 | After 1750 anthropogenic emissions have experienced exponential growth and starting around the 1850s, human-induced land-use change experienced close to linear growth. The natural sinks have experienced related exponential growth. Data points are from the Global Carbon Budget (Le Quéré et al., 2018) except where noted. Not all data points have values prior to 1860s. The ocean and atmospheric sinks have additional gaps starting in 2005 onward. The break for the atmospheric curve is completed by the overlay of the globally averaged Mauna Loa Keeling curve displaying anthropogenic emissions (value parts per million volume - 277 ppm) for the time period 1980-2017 and converted to GtC with the stock conversion factor of 2.12.

The Global Carbon Budget 2017's Equation:

$$E_{ff} + E_{luc} = G_{atm} + S_{ocean} + S_{land} + B_{bim}, \quad [1]$$

(Le Quéré et al., 2018) states the yearly growth of the fossil fuel and land-use change emissions are equal to the total yearly growth in CO_2 concentration for all natural sinks: atmosphere, ocean, and land sinks. This yearly growth rate equalling the natural sink yearly growth rate can be expanded to total cumulative emissions equalling the current anthropogenic carbon that is distributed to a natural sink. Where the GCB equation concerns yearly flux, equation [2] shows the cumulative emission sources are equal to the total anthropogenic carbon among the three sinks for a given year *n*:

$$E_{\Sigma ff_n} = \sum_{i=1750}^{n} E_{ff_i}, \quad [2]$$

$$E_{\Sigma ff_n} + E_{\Sigma luc_n} = A_{atm\ sink_n} + A_{ocean\ sink_n} + A_{land\ sink_n}. \quad [3]$$

From the equation, we can see the current total anthropogenic atmospheric CO_2 concentration is the total atmospheric CO_2 concentration minus the year 1750's CO_2 concentration of 277 ppm. Multiplying the current anthropogenic CO_2 ppm by 2.12 (Ballantyne et al., 2012) yields the anthropogenic carbon content in GtC.

The relationship between total carbon emitted and how it is distributed to each natural sink is shown in Figure 2, by stacked columns of cumulative anthropogenic fossil fuel and land-use change emission sources and Earth's three natural sinks. The negative quantity of the natural sinks shows the amount of carbon that ought to be removed to balance out the total amount of carbon emitted. The oceanic anthropogenic carbon is about roughly 58% of the atmospheric anthropogenic carbon or roughly 36% of the total emitted from fossil fuel emissions. The atmospheric anthropogenic carbon accounts for the remaining 63% of fossil fuel emissions.

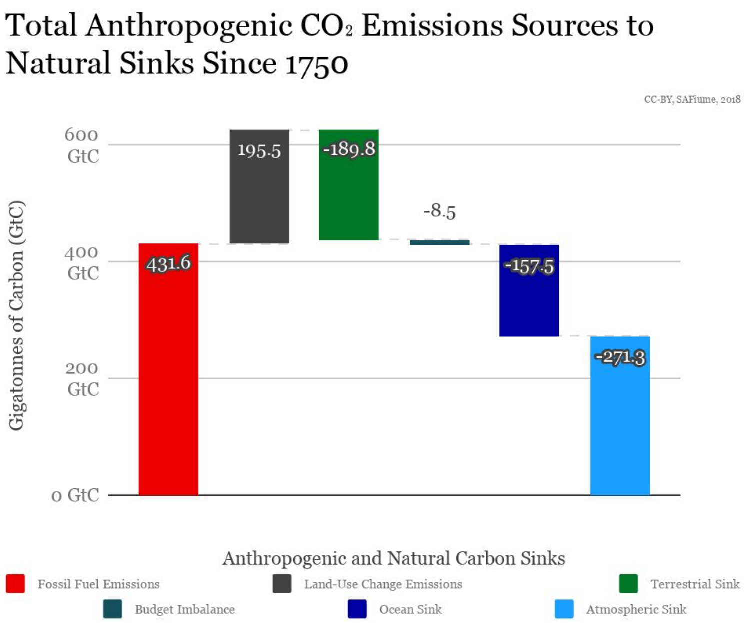

Figure 2 | Emissions sources are distributed nearly 36% to the ocean and 63% to the atmosphere, assuming Land-use change roughly equals the land sink. The budget imbalance is due to carbon missing from a natural sink, possibly from seasonal change and differing accounting methods.

Total anthropogenic carbon emissions experienced strongly accelerating growth compared to the stable historic CO_2 concentration. Figure 3 is a composite graph of CO_2 concentration data from multiple Antarctic ice cores studies performed on the Dome Concordia (Dome C) (Luethi et al., 2008; Flückiger et al., 2002; Monnin et al., 2001), Vostok Dome (Siegenthaler et al., 2005; Pépin et al., 2001; Petit et al., 1999;), Taylor Dome (Indermühle et al., 2000), WAIS Divide (Bauska et al., 2015), Maud Dome and the South Pole (Siegenthaler et al., 2017), and Law Dome (Etheridge et al., 1996; MacFarling Meure et al., 2006 and MacFarling Meure 2004), stretching for about two thousand years, from 600 BCE to 2004 CE and completed with the globally averaged CO_2 concentration from Mauna Loa from 1980 CE - 2017 CE, resulting in the top adjoined blue curves. This atmospheric curve has been shifted upwards to start above the top of the ocean sink curve. The mean CO_2 concentration of 280.9 ± 0.9 ppm for 600 BCE to 1750 CE, is shown in light green. The left axis has been calibrated to set 281 ppm equal to 348 GtC such that the green line meets 190 GtC - the top of the land curve added to 158 GtC - the top of the ocean curve. The curve in red is total anthropogenic emissions from both fossil fuel and land-use change. The dark blue and green lines are the ocean and land sinks respectively, which are cumulatively stacked below the atmospheric curve to illustrate the relationship to total carbon emissions. The top blue line doesn't meet the red emissions curve due to the budget imbalance.

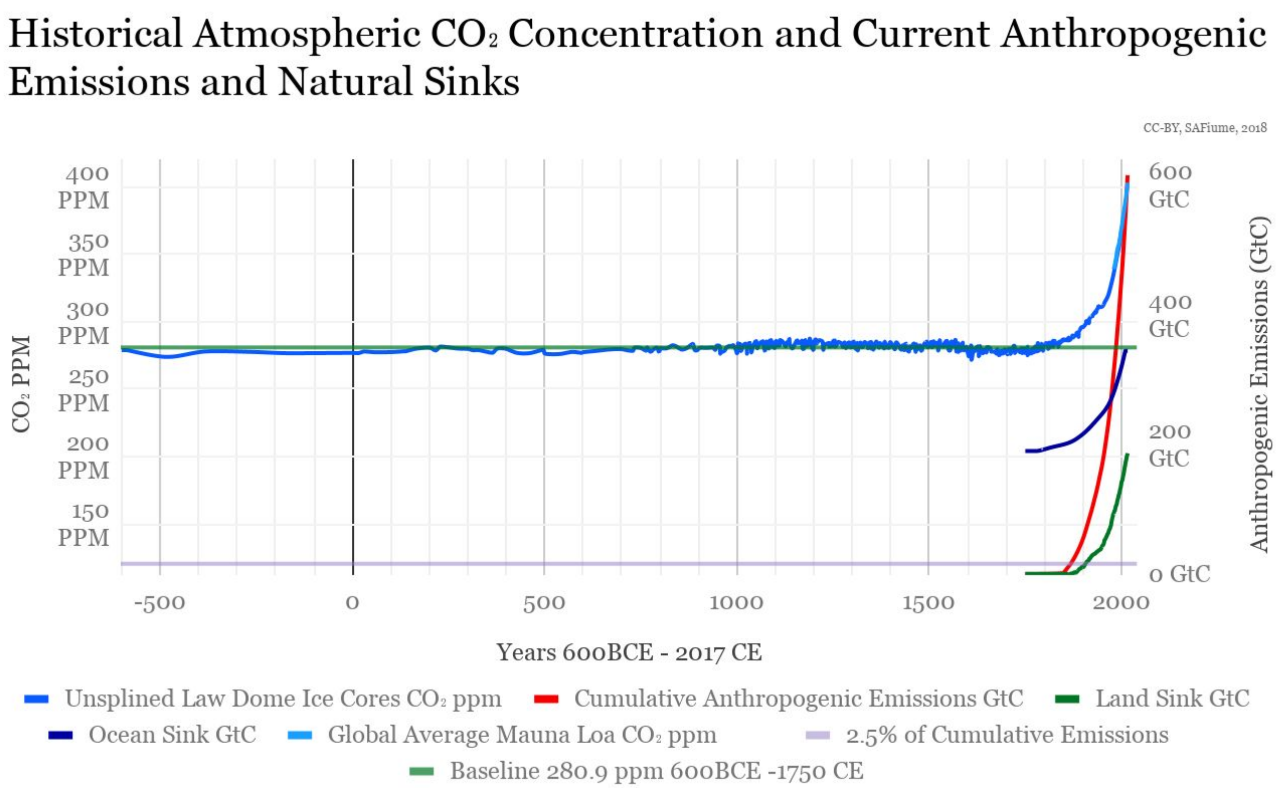

Figure 3 | Historical atmospheric CO_2 concentration is shown stacked above the ocean and land sink totals. The ice core CO_2 concentration data is from the Dome C (Monnin et al., 2001; Luthi et al., 2008), raw Law Dome data points (Etheridge et al., 1996; MacFarling Meure 2004; MacFarling Meure et al., 2006), WAIS Divide (Bauska et al., 2015), Maud Dome and the South Pole (Siegenthaler et al., 2017). Law Dome data from the present reads slightly lower ppm than Mauna Loa's global average. The data to generate the graphs are open and listed in Data Availability section. Cumulative anthropogenic emissions from fossil fuels and land-use change total 627 GtC and start picking up in the mid-1800s. The line in light purple is 2.5% of total emissions about 15.7 GtC. The light green line is the mean CO_2 concentration equaling 281 ppm from 600 BCE to 1750 CE. The axes are calibrated such that 113.18 ppm equates to 0 GtC of anthropogenic emissions increases.

The line in light purple corresponds to 2.5% of 627 GtC, or total anthropogenic emissions for both land-use and fossil fuel emission, equalling about 15.7 GtC, or 284 ppm.

The baseline of 277 ppm is the mean ppm for the time 1739 to 1772 CE. To check that this concentration was not a local minimum for only that time span the historical CO_2 concentration was examined and shown in Figure 4. Antarctic ice cores from Law Dome, Dome C, Maud Dome, Taylor Dome, WAIS Divide, Vostok and the South Pole yielded that CO_2 concentration has varied only slightly, ranging from 182.2 ppm to 287.5 ppm, for 137,000 BCE to 1750 CE. For modern times CO_2 concentration has been stable since 1750 back to about 600 BCE. Before 600 BCE, the concentration slowly trends lower than 275 ppm and eventually dropping to 184 ppm. A mean from the ice core samples gives a baseline of 280.9 ± 0.9 ppm for the recent stable past of 600 BCE to 1750 CE.

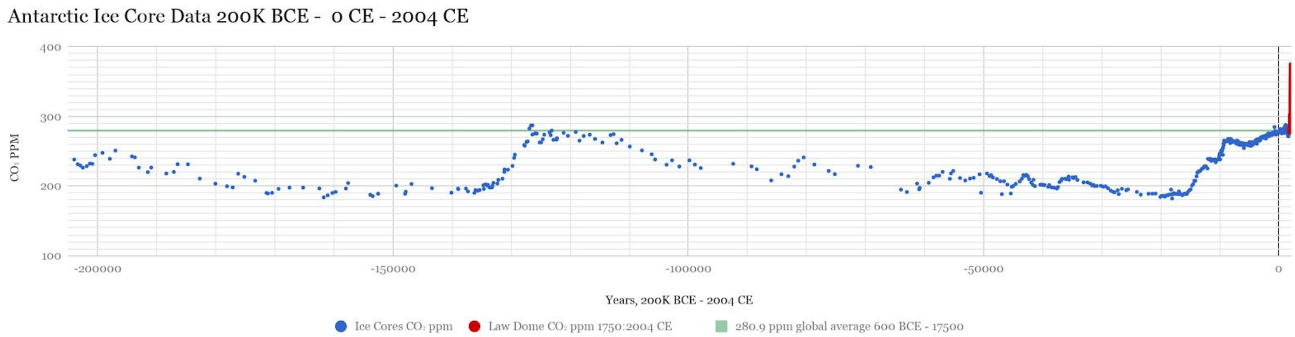

Figure 4 | Scatter plot of Antarctic Ice Core CO_2 concentration data from multiple ice cores: Law Dome, Dome C, Maud, Taylor Dome, WAIS Divide, Vostok and the South Pole from the time of 125000 BCE to 2004 CE. The pale green line is the mean of 280.9 from 600 BCE to 1750 CE.

Given the exponential forcing from the total cumulative emissions, the line in purple from Figure 3 represents a potential safe region to reduce major CO_2 concentration increase from outgassing. However, it's also possible the only safe region to prevent major CO_2 concentration increase from outgassing, is the total removal of all cumulative anthropogenic emissions since 1750.

3. Determining Carbon Dioxide to be Removed

By removing carbon dioxide from the atmosphere, we can change the atmospheric CO_2 concentration. If the total anthropogenic emissions were removed from the atmospheric sink equalling 271.3 GtC, given there are still hundreds of gigatonnes of carbon remaining in the other sinks outgassing and diffusion would transfer the CO_2 in the land and ocean sinks back to the atmosphere. Specifically, if we were to remove 271.3 GtC

$$627.1\ GtC\ -\ 271.3\ GtC\ =\ 355.8\ GtC, \quad [4]$$

or

$$431.6\ GtC\ -\ 271.3\ GtC\ =\ 160.3\ GtC, \quad [5]$$

we'd still have a remaining 356 GtC for the ocean plus land in equation [4], or 160 GtC assuming the land-use change is roughly equal to the land sink shown in equation [5]. Still assuming the land-use change is roughly the same as the land sink, the natural rebalancing would move atmospheric CO_2 concentration from 277 ppm upwards depending on how much the land sink outgasses. 160 GtC was last seen during 1980 when cumulative fossil fuel emissions were 164 GtC. After we reach a desired atmospheric concentration level, we need to continue to remove additional carbon dioxide to lower the anthropogenic carbon diffused in the ocean surface waters.

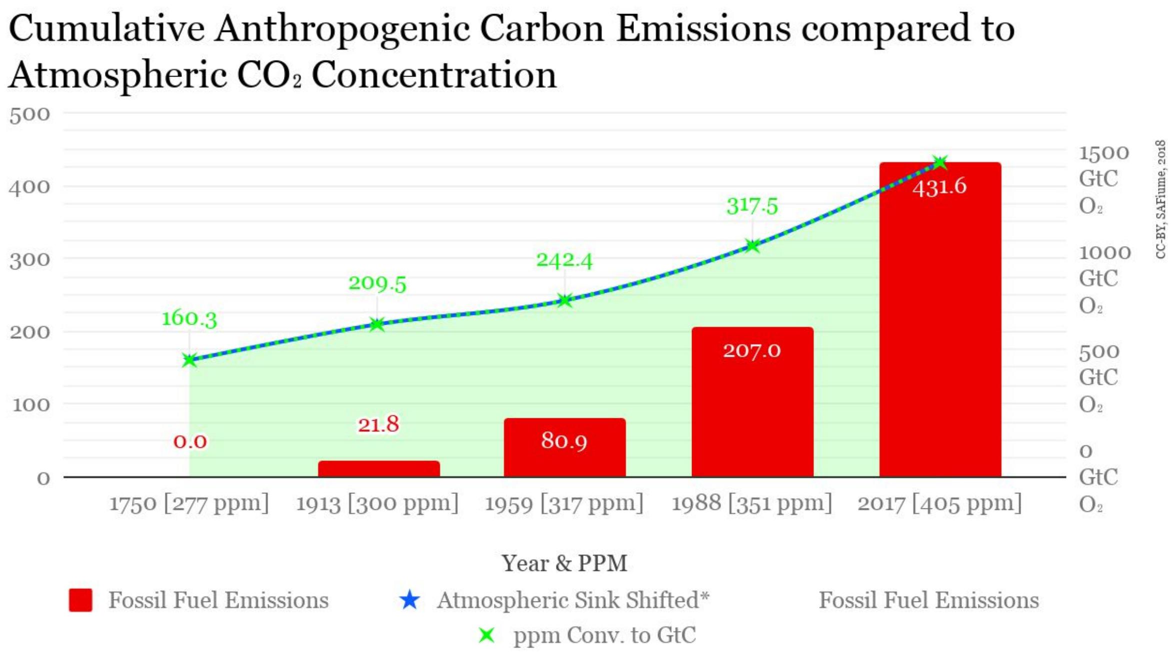

Figure 5 | Fossil Fuel Emissions and CO_2 ppm concentration converted to GtC for the years, 1750, 1913, 1959, 1988, 2017. The horizontal axis scaling isn't to scale and hides the true exponential extent of these curves. The ppm curve in green closely matches the global average CO_2 concentration when converted to GtC. Atmosphere shifted data points for 1998, and 2017 are from the Mauna Loa yearly global average CO_2 ppm minus 277 ppm converted to GtC.

Figure 5, shows the atmospheric curve in blue is very close to the CO_2 concentration in ppm converted to GtC, shown in green. The curves are practically equal as anthropogenic atmospheric CO_2 is atmospheric CO_2 ppm - 277 ppm.

For illustration purposes, we'll examine a common target of 350 ppm. 350 ppm was roughly seen in 1988 when atmospheric emissions were about 317 GtC, or if starting from now equals a removal of

$$431.6\ GtC\ -\ 317.5\ GtC\ =\ 114.1\ GtC. \qquad [6]$$

The data point for 351 ppm is shown 114.1 GtC lower than 431.6 GtC in Figure 5. If we remove 114.1 GtC shown in equation [6], the atmosphere would likely increase upwards above 350 ppm, from the ocean and possibly land outgassing.

To more accurately affect and remove carbon deposited to all sinks, we refer to the historical anthropogenic concentrations for each sink. To illustrate how to determine how much carbon to remove, find the year the desired ppm or emissions occurred, then take the current cumulative emissions and subtract the historical cumulative emissions for that year. For 350 ppm, the actual removal should be as shown in equation [7],

$$431.6\ GtC\ -\ 207.0\ GtC\ =\ 224.6\ GtC. \qquad [7]$$

Note, that 350 ppm is significantly far from the baseline of 280.9 ppm and which represents about 207 gigatonnes of carbon that wasn't previously in the atmosphere or oceans since the mid-Pliocene warm period or about 3.2 MyBP (million years before present, or million years since 1950 CE) (Raymo et al., 1992).

Figure 6 shows the cumulative stacking of all natural sinks and emissions sources for five individual years. The ppm curve is the same as above, and like above practically overlays the atmospheric curve. The atmospheric sink in the dashed blue line has been upshifted by the final total of the ocean sink (157.5 GtC) to show total growth in sinks from emissions. The ocean and land sink show very similar growth rates. The exponential increase in emissions radically increases the amount of carbon that ought to be removed to stabilize Earth’s climate.

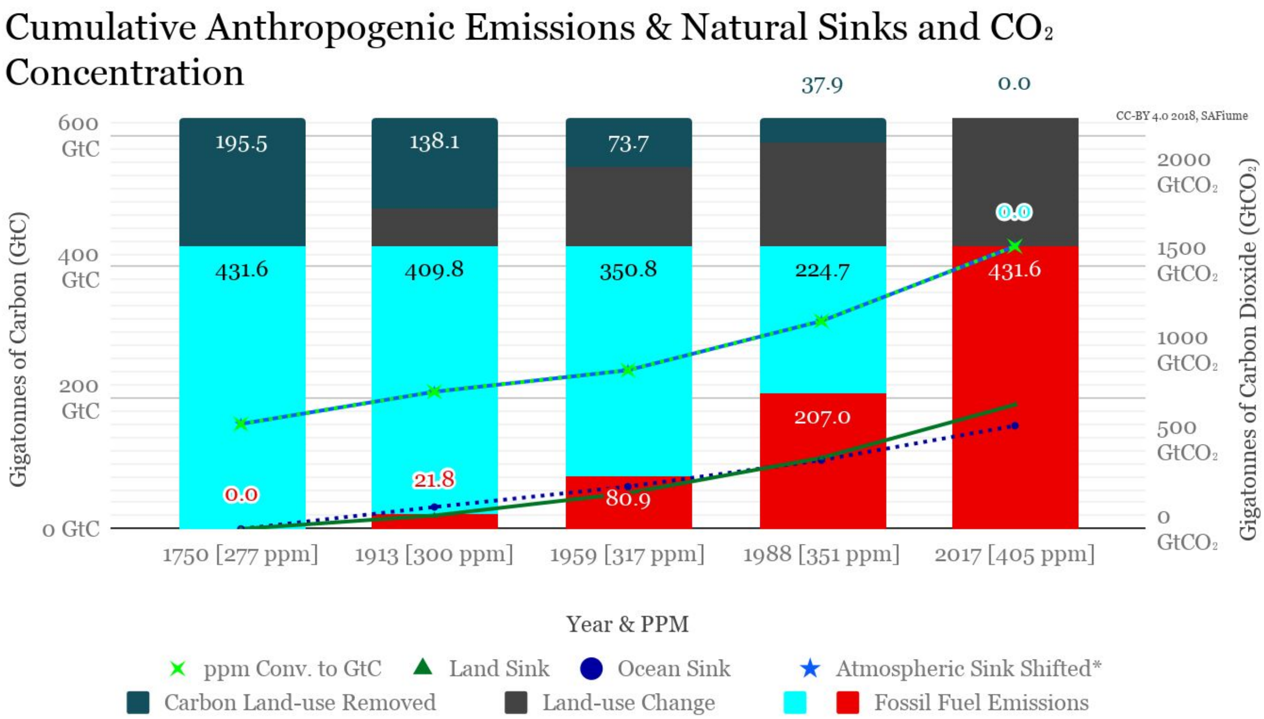

Figure 6 | This graph shows a conversion of ppm to GtC shifted to descend from 431.6 GtC, and the rate increase for the natural sinks over time. It has stacked columns of fossil fuel, land-use change emissions, and carbon removal targets for the years, 1750, 1913, 1959, 1988, and 2017, corresponding to 277, 300, 317, 351, 405 ppm, and natural sink growth. CO_2 ppm concentration is converted to GtC. The Carbon Removal is the total amount of carbon that would have to be removed to restore the carbon dioxide concentration in all sinks and emissions for that time. If we remove a total of 409.8 GtC and also 174 GtC from land-use change emissions, we would achieve 300 ppm last seen in 1913.

‘We infer from Cenozoic data that CO_2 was the dominant Cenozoic forcing, that CO_2 was ~450 ± 100 ppm when Antarctica glaciated, and that glaciation is reversible.’ (Hansen et al., 2008) The error margin of 100 ppm is wide enough to place reversing glaciation possible at 350 ppm. Given the radical nature of the exponential increase from 277 ppm and temperature increase from pre-industrial times, 350 ppm isn’t likely to yield a long-term stable climate.

Given the magnitude of outgassing by the three sinks, effort should focus on removal of total cumulative anthropogenic carbon for a given time period to achieve a specific CO_2 concentration, not only by the conversion of ppm to GtC for the atmospheric sink. To achieve 277 ppm, focus on removing total cumulative anthropogenic emissions, all 431.6 GtC (approximately 1.5 trillion tonnes CO_2) and forcing the land sink to zero emissions, not by just removing 272 GtC (approximately 1 trillion tonnes of CO_2).

3.1 Comparison with Yearly Change

To better visualize the magnitude of growth in total emissions, total cumulative carbon emissions were graphed opposed to the year to year change in emissions. In comparison Figure 7 shows the yearly change of emissions more commonly seen in papers comparing the Shared Socioeconomic Pathways (SSPs)(Riahi, et al., 2016). The yearly change graph hides the true exponential nature of emissions curves and doesn’t easily show how much carbon may need to be removed to restore climate to a desired emissions target. For illustration in Figure 7, the SSP1 IMAGE RCP 2.6 by the IMAGE group (van Vuuren, 2016) was modeled in yellow with the existing sinks and emissions data as well as four possible hypothesis emission declines to zero cumulative emissions. The SSP1 IMAGE RCP 2.6 is the marker scenario for SSP1: under this scenario, CO_2 along with all other GhG emissions peak gradually and then drop (SSP Public Database version 1.1, 2018, van Vuuren, 2016). The SSP1 IMAGE RCP 2.6 emissions data spline was extrapolated from the emissions per decade starting from 2010 to 2100 and including emissions from 2005 as listed from the SSP database. Radiative forcing can be converted to CO_2 concentration by rearranging of formula [8] (Wikipedia, 2018) to formula [9]:

$$\Delta F_{year} = (5.35 * ln\frac{CO_2\,ppm}{277})Wm^{-2}, \qquad [8]$$

$$277 * exp(\frac{\Delta F_{year}\,Wm^{-2}}{5.35}) = CO_2\,ppm, \qquad [9]$$

The newer RCP 1.9 data wasn't available at the time of this paper. RCP 2.6 sets radiative forcing at 2.6 W/m^2,

$$277 * exp(\frac{2.6\,Wm^{-2}}{5.35}) = 450.34\ eq\ ppm. \qquad [10]$$

which is roughly 450 ppm of CO_2-eq as shown in equation [10]. Actual CO_2 ppm would be lower at about 376 ppm, due to forcing circa 2005, shown in equation [12], or 2004, shown in equation [11] which was according to the formula for radiative forcing rounded to 1.63 W/m^2 (NOAA, 2016), as shown in equation [13] :

$$\Delta F_{2004} = 2.5960 = 1.627 + 0.483 + 0.159 + 0.174 + 0.063 + 0.09, \qquad [11]$$

$$\Delta F_{2005} = 2.6260 = 1.655 + 0.481 + 0.162 + 0.173 + 0.063 + 0.092, \qquad [12]$$

$$277 * exp(\frac{1.627}{5.35}) = 375.45\ ppm. \qquad [13]$$

For a comparison, Mauna Loa globally average was 376.78 ppm for 2004 and 378.81 ppm for 2005 (Dlugokencky et al., 2018), Law Dome spine read 374.6 ppm for 2004 (Etheridge et al., 1996; 2010). For the SSP1 IMAGE RCP 2.6 CO_2 radiative forcing ends at 2.355 W/m^2 by 2100 (SSP Public Database version 1.1, 2018).

In Figure 7, it's not readily apparent what cumulative emissions will be at the end of the RCP and emission declines. Our hypotheses emissions declines drop down to zero cumulative emissions in 2040, and 2100 (shown in detail in Figure 8), whereas the IMAGE SSP1 RCP 2.6 drops cumulative fossil fuel emissions down to about 870 GtC, roughly equivalent to total radiative forcing 2.6 and holding carbon dioxide concentrations to about 430 ppm by the end of 2100.

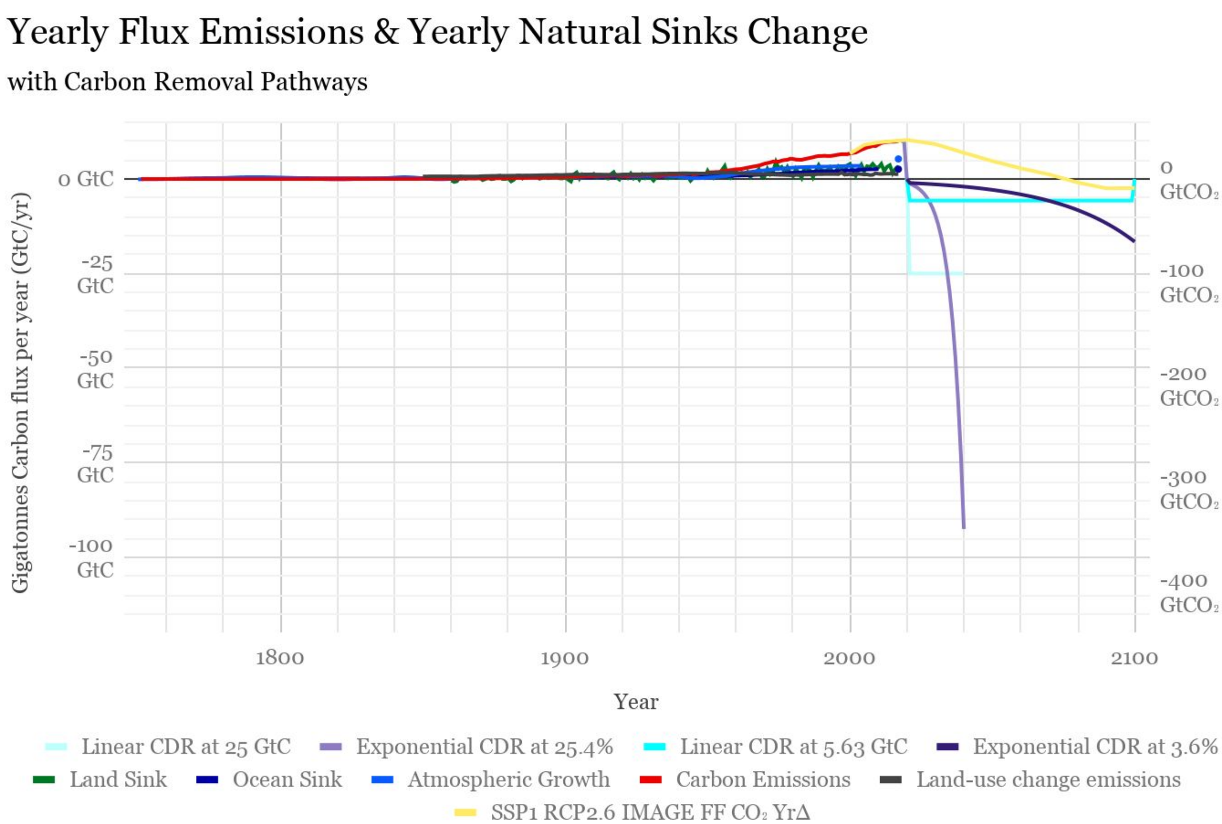

Figure 7 | This is the yearly graph of emissions and sinks change. Included are the emission declines for carbon removal to achieve zero cumulative emissions. Most of the standard SSPs cross zero GtC after 2040 and end by 2100 or later. The SSP1 RCP26 IMAGE shows Fossil Fuel CO_2 emissions from the SSP database. The SSPs reach the warming target of 2ºC to 1.5ºC above Earth's temperature since 1860s. The SSPs only remove some portion of carbon to equal the given radiative forcing and not all anthropogenic emissions. Although SSP1 IMAGE RCP 2.6 drops below zero yearly emissions it doesn't reach zero cumulative emissions.

SSP1 IMAGE was modeled using MAGICC 6.0 (Meinshausen, M. 2011) which internally starts cumulative emissions from 1765 CE. Figure 8 lists SSP1 IMAGE RCP 2.6 yearly cumulative fossil fuel emissions change modeled on cumulative fossil fuel starting from levels in 2000. It also uses the extrapolated emissions data spline for SSP1 IMAGE RCP 2.6 like in Figure 7. All the emission declines and the SSP are direct carbon dioxide fossil fuel emissions, and not the combined GhGs: CO_2-eq. Under the newer RCP 1.9, CO_2 emissions could be as low as 184.3 GtC corresponding to CO_2 forcing of 1.14 seen in 1984 (NOAA, 2016). Although 184.3 GtC is less than 207 GtC (cumulative fossil fuel emissions at 1988, and 351 ppm), it is still a magnitude larger than 21.8 GtC.

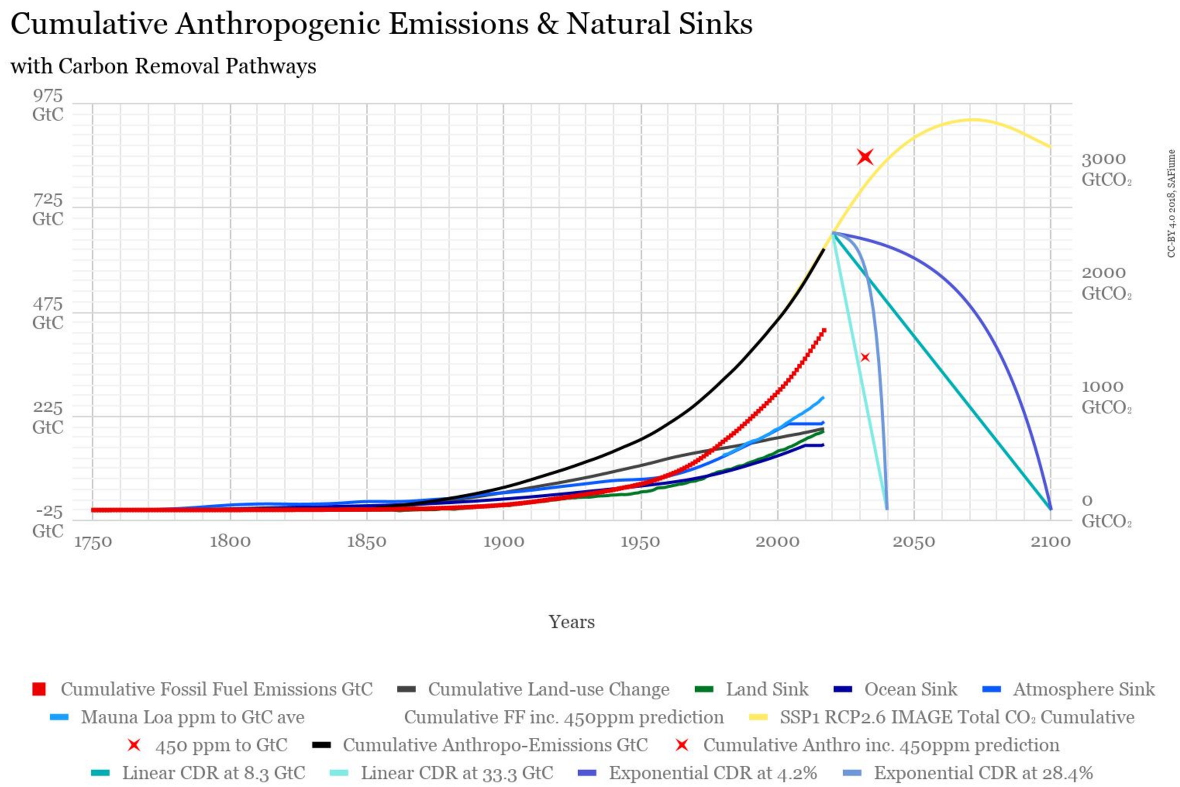

Figure 8 | Also included is the marker scenario for SSP 1: IMAGE RCP 2.6 shown in yellow line. IMAGE RCP 2.6 scenario ends with a radiative forcing of 2.624, and 430 ppm CO_2-eq (SSP Public Database version 1.1, 2018). The IMAGE-RCP 2.6 for only fossil fuel emissions is about 415 ppm by 2100. Given the variance in short forcing GhG, actual CO_2 ppm could be as low as the historic concentration of about 376 ppm, due to the radiative forcing for only CO_2 circa 2005, or 2004 => 277 * exp(1.63/5.35) = 376.

Given exponential forcing of emissions, some small region starting at 277 ppm possibly up to 300 ppm is likely to lead to a stable climate where little to no outgassing from the other sinks. 300 ppm (last seen in 1913 when fossil fuel emissions were 22 GtC, and land-use change was 57 GtC) and less should be investigated to find the determining factor or Earth system configuration for climate stability. The investigation model or hypothetical should be able to set carbon concentration simultaneously within all sinks: atmosphere, ocean and land, and also model large volume carbon removal over time spans of ultrashort, short, medium and long time frames.

Since the direct consequence of lowering CO_2 concentration results in outgassing and as the fossil fuel emission curve is a steep exponential of growing carbon, climate stability is likely with a very low to zero percentage of fossil fuel emissions. If verified, nearly all, or the cumulative total amount of carbon from fossil fuel emissions, should be removed from ocean surface water and atmosphere sinks before we can see a stable climate. By removing the total amount of carbon it should additionally force the ocean sink to become more alkaline compared to the present, and should hopefully, return natural albedo cooling and natural restoration of the cryosphere.

As the originating source emissions and subsequent natural sinks are exponentially increasing, at our current growth rate of 2% per year we have a little over 14 years before hitting 450 ppm as shown in Figure 8. This extrapolation is based on continued fossil fuel emissions at a 2% yearly growth rate and extrapolating the time it takes for the atmospheric sink to reach 450 ppm, shown in the little red X, and also to the black cumulative fossil fuel plus land-use change curve shown in the large red X. As the extrapolation only considers anthropogenic emissions increases and doesn't take into account likely exponential warming from the loss of the Greenland Ice sheet and unlocking of frozen methane in the permafrost, a more realistic projection is likely much sooner than 14 years. We have little time to hit peak yearly emissions, and then to hit zero yearly emissions.

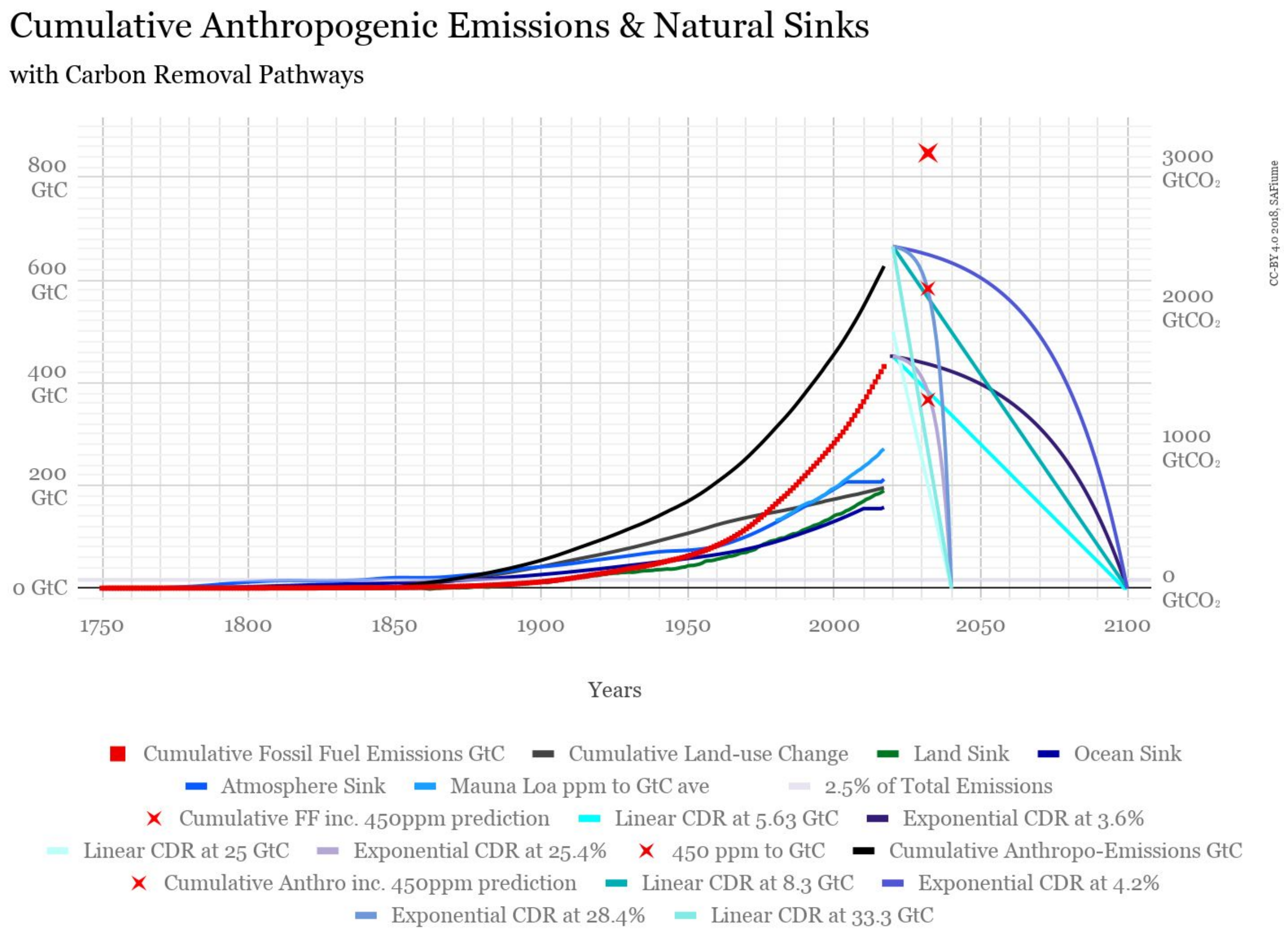

Figure 9 | Cumulative Anthropogenic Emissions & Natural Sinks and emission declines to zero cumulative emissions. 450 ppm is extrapolated from the Mauna Loa curve and shown in the red X. Translating that extrapolation to the fossil fuel and fossil fuel plus land-use curves assuming a continued yearly growth rate of 2% gives the red Xes. The red Xes are reached by 2032. The emissions declines bound CDR in a minimum and maximum effort range to target what's possible, and don't account for a price on carbon or price to deploy a given technology which is embedded in some Pathway models. Efforts that are between the teal and purple lines would keep climate radically below 1.5ºC. Efforts between the teal and purple lines that end at something less than 20 GtC would reset climate levels prior to the climate of the early 1900s. Efforts that reach zero and are between the teal and purple lines would reset the climate back to levels last seen in 1750.

4. Possible Emission Declines to Zero Degrees Warming

Four hypothetical emission declines are presented to show linear and exponential declines to bound removal in a minimum and maximum timeframe. In Figure 9, zero degrees warming emission decline can be achieved by the curves in shades of cyan or purple. A possible maximum cumulative emissions removal is shown spanning eighty years. The cyan line is a hypothetical linear carbon removal of 5.8 GtC year $^{-1}$ for eighty years, starting at 500 GtC. By 2080, there would only be about 115 GtC left to remove. Depending on how the CO_2 concentration was split between the sinks, the oceans should see significant recovery as well as slight global cooling by 2080. The dark purple curve shows an exponential decline of 3.5% starting from 461 GtC in 2020 finally trending to below zero in 2100.

For climate restoration in less than half a human lifespan, the pale lines show hyper-aggressive carbon removal in 20 years. The pale purple shows an exponential decline of 27.5% starting from 461 GtC in 2020 finally trending to below zero in 2040. The pale cyan shows a linear removal of 25 GtC year $^{-1}$ for twenty years, and 125 GtC would be remaining at year 15. How fast the oceans recover, or permafrost regenerates in response to an abrupt drop in CO_2 concentration should be explored. In an abrupt CO_2 concentration drop scenario, solid carbon could additionally be distributed to the land sink, to keep the land sink absorption high.

These emission declines are a simple removal of carbon and don't take into account a price for carbon or price to implement a given carbon removal method which is in some of the advanced modeling tools for analyzing Pathways. These simpler declines show a rough guideline of what we can remove, and provide a rough check for the model output, whereas the more advanced modeling tools forecast where we are in comparison to Earth's climate. At the time of this paper, a model output of complete climate restoration was unavailable, necessitating this paper.

The exponential declines mimics a slow exponential increase of reduction in carbon emissions. Exponential curves are more similar to a rapid technology adoption model, or crash in price from technological improvements and follow Moore's Law.

5. Data Availability

All data and graphs are available in the open google spreadsheet: Total Emitted Carbon Graphs and Comparisons. The tabs contain SCEN data that can be converted to CSV files to be imported to MAGICC. The hypothetical declines were imported to MAGICC 6.4 and live.magic.org to allow a finer detailed comparison. The MAGICC 6.x SCEN files for declines are available at the: google drive location. SSP1 IMAGE RCP 2.6 data was obtained at the SSP Public Database version 1.1 and generated in 2018. This paper is open and licensed under the Creative Commons CC-BY 4.0 International License.

6. Conclusion

Creating CDR targets from cumulative emissions totals should quicken climate restoration of the polar regions as they focus on removal of emissions rather than holding to a given warming level. Emissions diffused in surface waters and it's complex interaction with ocean mixing and the atmospheric sink justifies a more involved approach to generating CDR targets, rather than a plain conversion of atmospheric ppm to bulk carbon. The exponential nature of cumulative growth in emissions, though obscured when only considering a radiative forcing level or purely looking at the yearly change in emissions, shows significant growth throughout the 1980s to the present, mirrors much of the deployment growth of information advances. Given the exponential nature and magnitudes larger than zero cumulative emissions, the effects of CDR to 22 GtC fossil fuel added to 57 GtC land-use change ranging to CDR to zero cumulative emissions with shorter than 80 year timeframes or ending in the year 2100, would highly benefit from additional study. Given the vast amounts of carbon that needs to be removed for complete climate restoration, carbon dioxide removal technologies: geo-engineering, bio-engineering, and others engineering and processes comprising negative emissions technologies, and natural processes, should aid the existing portfolio of technologies, processes, and policies, such as, renewables, non-fossil fuels, clean nuclear, energy storage, and phase-out of fossil fuels, etc., to seek peak and zero emissions, and ultimately climate restoration. The sooner we hit peak followed by zero yearly emissions; the less CO_2 we have to remove. All efforts should be made to hit peak followed by zero yearly emissions as soon as possible, to start the removal of potentially more than 1.5 trillion tonnes of carbon dioxide.

7. Error and Uncertainties

All measured data has an uncertainty up to one standard deviation. Uncertainty for the cumulative anthropogenic fossil fuel emissions is ± 5% from the Global Carbon Budget 2017 (Le Quéré et al., 2018) and CDIAC (Boden et al., 2017). '*Generally, […] mature economies […] have uncertainties of a few percent[s] while developing countries such as China have uncertainties around ± 10%.*' (Le Quéré et al., 2018). Overall a medium confidence was given to the fossil fuel emissions dataset, as it was generated indirectly from energy data (Durant et al., 2011) and includes per country data variation. Land-use change emissions uncertainty is estimated at ± 0.7 GtC yr^{-1} and was assigned a low confidence due to *'the inconsistencies among estimates and the difficulties to quantify some of the processes in DGVMs'* (Le Quéré et al., 2018). For the natural sinks: the land sink uncertainty for the Dynamic Global Vegetation Models (DGVMs) averages to ±0.8 GtC yr^{-1} from 1959 to 2016 and has a medium confidence level. The ocean surface water sink uncertainty yearly change is ±0.5 GtC and given a medium confidence. The atmospheric annual growth uncertainty is has a mean of 0.61 GtC yr^{-1} for 1959-1979, and 0.19 GtC yr^{-1} for 1980-2016, and was given a high confidence given the direct measurements comprising the datasets. The historical atmospheric CO_2 concentration from 1750-1959 has an uncertainty of ±3 ppm converted to $\pm 1\sigma$, from the Law Dome ice core data (Joos et al., 2008).

The 1980 - 2017 CO_2 concentration from Mauna Loa provided by NOAA/ESRL is listed with an uncertainty of 0.10 ppm. Antarctic Law Dome ice core data spline has an uncertainty of 1.2 ppm for 1-2004 CE (Etheridge et al., 1996; 2010), and individual ice core samples at 1.1 ppm for 1-1996 CE (MacFarling Meure et al., 2006). The Antarctic ice core data points for EPICA Dome Concordia (Dome C) (Monnin et al., 2001; Luthi et al., 2008), Vostock (Petit et al., 1999; Pépin et al., 2001; Siegenthaler et al., 2005; Luthi et al., 2008), Taylor Dome (Indermühle et al., 2001), WAIS Divide (Bauska et al., 2015), Maud Land and the South Pole (Siegenthaler et al., 2017), have uncertainty ranging from .1 ppm up to 2.62 ppm, a mean uncertainty of 0.8 ppm. For convenience, the combined datasets and individual uncertainties are listed in the Antarctic Historicals and graph tabs in the spreadsheet Total Emitted Carbon Graphs and Comparisons (Fiume, 2018).

The CO_2 concentration baseline of 280.9 ppm from 600 BCE to 1750 CE has an average uncertainty of 0.9 ppm for the non-splined ice core data points from Dome C (Monnin et al., 2001; Luthi et al., 2008), Law Dome (Etheridge et al., 1996; MacFarling Meure et al., 2006), WAIS Divide (Bauska et al., 2015), Maud Dome and the South Pole (Siegenthaler et al., 2017). The Mauna Loa records show slightly elevated concentrations over the modern Law Dome readings and as a precaution, lowers the confidence level slightly to medium-high.

8. Competing Interests

Shannon Fiume runs Open NanoCarbon (received $100 USD, in total donations) a presently unfunded non-profit effort doing open science research and development to solidify carbon from atmospheric CO_2, with the charter to enable complete climate restoration by removal of total anthropogenic emitted carbon dioxide.

9. Acknowledgments

The Global Carbon Budget has been instrumental in writing this paper and its inspiration. Shannon thanks the GCB authors, NOAA and CSIRO for the ice core data and Scripps and NSF, Earth Network, for Mauna Loa data. Shannon additionally thanks the Open NanoCarbon Anonymous donor, Matt Eshed, Susan Lee, Peter Fiekowsky, Eric Harley, Andy Lee and everyone who's commented on the paper, and those working to restore the climate.

10. References

1. Ballantyne, A.P., Alden, C.B., Miller, J.B., Tans, P.P., and White, J.W.C., (2012), Increase in observed net carbon dioxide uptake by land and oceans during the past 50 years., *Nature*, **488**, pp. 70–72 (02 August 2012), DOI: 10.1038/nature11299
2. Bauska, T.K.; Joos, F.; Mix, A.C.; Roth, R.; Ahn, J.; Brook, E.J. (2015), Links between atmospheric carbon dioxide, the land carbon reservoir and climate over the past millennium, *Nature Geoscience*, **8**, pp. 383–387, DOI: 10.1038/ngeo2422,
    a. (https://www1.ncdc.noaa.gov/pub/data/paleo/icecore/antarctica/wais2015co2.txt),
    b. https://www.ncdc.noaa.gov/paleo-search/study/18316
3. Boden, T.A., Andres, R.J., Marland, G., (2017), Global, Regional, and National Fossil-Fuel CO_2 Emissions, (http://cdiac.ornl.gov/trends/emis/overview_2014.html), Carbon Dioxide Information Analysis Center, Oak Ridge National Laboratory, Department of Energy, Tennessee
4. Dlugokencky, E., Tans, P., and Keeling R., (2018), Mauna Loa Globally Averaged Yearly CO_2 ppm, Earth Science Research Laboratory, National Oceanic and Atmospheric Administration, Scripps Institution of Oceanography
    a. http://www.esrl.noaa.gov/gmd/ccgg/trends/, ftp://aftp.cmdl.noaa.gov/products/trends/co2/co2_annmean_gl.txt,
5. Durant, A. J., Le Quéré, C., Hope, C., and Friend, A. D., (2011), Economic value of improved quantification in global sources and sinks of carbon dioxide, *Phil. Trans. A,* **369**, pp. 1967-1979, DOI: 10.1098/rsta.2011.0002
6. Etheridge, D.M., Steele, L.P., Langenfelds, R.L., Francey, R.J., Barnola, J.-M. and Morgan, V. I. (1996), Natural and anthropogenic changes in atmospheric CO_2 over the last 1000 years from air in Antarctic ice and firn, *J. Geophys. Res.*, **101(D2)**, pp. 4115–4128, DOI: 10.1029/95JD03410
7. Etheridge, D.M. et al. (2010), Law Dome Ice Core 2000-Year CO_2, CH_4, and N_2O Data, IGBP PAGES/World Data Center for Paleoclimatology, Data Contribution Series # 2010-070, NOAA/NCDC Paleoclimatology Program, Boulder CO, USA
    a. http://cdiac.ess-dive.lbl.gov/trends/co2/ice_core_co2.html ftp.ncdc.noaa.gov/pub/data/paleo/icecore/antarctica/law/law2006.txt
8. Fiume, S., (2018), Total Emitted Carbon Graphs and Comparisons
9. Flückiger, J., Monnin, E., Stauffer, B., Schwander, J., Stocker, T. F., Chappellaz, J., Raynaud, D., and Barnola, J.-M., (2002), High-resolution Holocene N_2O ice core record and its relationship with CH_4 and CO_2, *Global Biogeochem. Cycles*, **16(1)**, pp. 10-1-10-8, DOI: 10.1029/2001GB001417
10. Hansen, J., Sato, M., Kharecha, P., Beerling, D., Berner, R., Masson-Delmotte, V., Pagani, M., Raymo, M., Royer, D. L., and Zachos, J. C., (2008), Target Atmospheric CO_2: Where Should Humanity Aim?, *The Open Atmospheric Science Journal* , **2**, pp. 217-231, DOI: 10.2174/1874282300802010217

11. Indermühle, A., Monnin, E., Stauffer, B., Stocker, T.F., Wahlen, M. (2001), Atmospheric CO_2 concentration from 60 to 20 kyr BP from the Taylor Dome Ice Core, Antarctica. *Geophysical Research Letters*, **27(5)**, pp. 735-738, DOI: 10.1029/1999GL010960
12. Joos, F. and Spahni, R., (2008), Rates of change in natural and anthropogenic radiative forcing over the past 20,000 years, *Proceedings of the National Academy of Science*, **105(5)**, pp. 1425-1430, DOI: 10.1073/pnas.0707386105
13. Le Quéré, C., Andrew, R. M., Friedlingstein, P., Sitch, S., Pongratz, J., Manning, A. C., Korsbakken, J. I., Peters, G. P., Canadell, J. G., Jackson, R. B., Boden, T. A., Tans, P. P., Andrews, O. D., Arora, V. K., Bakker, D. C. E., Barbero, L., Becker, M., Betts, R. A., Bopp, L., Chevallier, F., Chini, L. P., Ciais, P., Cosca, C. E., Cross, J., Currie, K., Gasser, T., Harris, I., Hauck, J., Haverd, V., Houghton, R. A., Hunt, C. W., Hurtt, G., Ilyina, T., Jain, A. K., Kato, E., Kautz, M., Keeling, R. F., Klein Goldewijk, K., Körtzinger, A., Landschützer, P., Lefèvre, N., Lenton, A., Lienert, S., Lima, I., Lombardozzi, D., Metzl, N., Millero, F., Monteiro, P. M. S., Munro, D. R., Nabel, J. E. M. S., Nakaoka, S.-I., Nojiri, Y., Padin, X. A., Peregon, A., Pfeil, B., Pierrot, D., Poulter, B., Rehder, G., Reimer, J., Rödenbeck, C., Schwinger, J., Séférian, R., Skjelvan, I., Stocker, B. D., Tian, H., Tilbrook, B., Tubiello, F. N., van der Laan-Luijkx, I. T., van der Werf, G. R., van Heuven, S., Viovy, N., Vuichard, N., Walker, A. P., Watson, A. J., Wiltshire, A. J., Zaehle, S., and Zhu, D. (2018), Global Carbon Budget 2017, *Earth System Science Data*, **10**, pp. 405-448, DOI: 10.5194/essd-10-405-2018
14. Luthi, D., Le Floch, M., Bereiter, B., Blunier,T., Barnola, J.-M., Siegenthaler, U., Raynaud, D., Jouzel, J., Fischer, H., Kawamura, K., and Stocker, T.F., (2008), High-resolution carbon dioxide concentration record 650,000-800,000 years before present, *Nature*, Vol. **453**, pp. 379-382, DOI: 10.1038/nature06949, https://www1.ncdc.noaa.gov/pub/data/paleo/icecore/antarctica/epica_domec/edc-co2-2008.txt
15. MacFarling Meure, C. (2004), The variation of atmospheric carbon dioxide, methane and nitrous oxide during the Holocene from ice core analysis, (Google Scholar), Ph.D. thesis, Univ. of Melbourne, Melbourne, Vic., Australia
16. MacFarling Meure, C., Etheridge, D., Trudinger, C., Steele, P., Langenfelds, R., van Ommen, T., Smith, A. and Elkins, J., (2006), Law Dome CO_2, CH_4 and N_2O ice core records extended to 2000 years BP, *Geophys. Res. Lett.*, **33**, pp. L14810, DOI: 10.1029/2006GL026152
17. Meinshausen, M., Raper, S. C. B., and Wigley, T. M. L., (2011), Emulating coupled atmosphere-ocean and carbon cycle models with a simpler model, MAGICC6 – Part 1: Model description and calibration, *Atmos. Chem. Phys.*, **11**, 1417-1456, DOI: 10.5194/acp-11-1417-2011
18. Meinshausen, M., Wigley, T. M. L., and Raper, S. C. B., (2011), Emulating atmosphere-ocean and carbon cycle models with a simpler model, MAGICC6 – Part 2: Applications, *Atmos. Chem. Phys.*,**11**, 1457–1471, DOI: 10.5194/acp-11-1457-2011
19. Monnin, E., Indermühle, A., Dällenbach, A., Flückiger, J., Stauffer, B., Stocker, T. F., Raynaud, D. and Barnola,J.-M., (2001), Atmospheric CO_2 concentrations over the Last Glacial Termination, *Science*, **291**, pp. 112–114, DOI: 10.1126/science.291.5501.112
20. National Oceanic and Atmospheric Administration (NOAA), (2016), The NOAA Annual Greenhouse Gas Index
    a. www.esrl.noaa.gov/gmd/aggi, https://www.epa.gov/sites/production/files/2016-08/climate-forcing_fig-1.csv
21. Pépin, L., Raynaud, D., Barnola, J.-M., and Loutre, M.F., (2001), Hemispheric roles of climate forcings during glacial-interglacial transitions as deduced from the Vostok record and LLN-2D model experiments, *Journal of Geophysical Research*, **106 (D23)**, pp. 31,885-31,892, DOI: 10.1029/2001JD900117

22. Petit, J.R., Jouzel, J., Raynaud, D., Barkov, N.I., Barnola, J.-M., Basile, I. , Benders, M., Chappellaz, J., Davis, M., Delayque, G., Delmotte, M., Kotlyakov, V.M., Legrand, M., Lipenkov, V.Y., Lorius, C., Pépin, L., Ritz, C., Saltzman, E., and Stievenard, M., (1999), Climate and atmospheric history of the past 420,000 years from the Vostok ice core, Antarctica, *Nature*, **399**, pp. 429-436, DOI: 10.1038/20859
23. Raymo, M.E, Grant, B., Horowitz, M., and Rau, G. H., (1992), Mid-Pliocene warmth: stronger greenhouse and stronger conveyor, *Marine Micropaleontology*, **27**, pp. 313-326, DOI: 10.1016/0377-8398(95)00048-8
24. Riahi, K., van Vuuren, D.P., Kriegler, E., Edmonds, J., O'Neill, B.C., Fujimori, S., Bauer, N. Calvin, K., Dellink, R., Fricko, O., Lutz, W., Popp, A., Cuaresma, J.C., KC, S., Leimbach, M., Jiang, L., Kram, T., Rao, S., Emmerling, J., Ebi, K., Hasegawa, T., Havlik, P., Humpendöder, F., Da Silva, L.A., Smith, S., Stehfest, E., Bosetti, V., Eom, J., Gernaat, D., Masui, T., Rogelj, J., Strefler, J., Drouet, L., Krey, V., Luderer, G., Harmsen, M., Takahashi, K., Baumstark, L., Doelman, J.C., Kainuma, M., Klimont, Z., Marangoni, G., Lotze-Campen, H., Obersteiner, M., Tabeau, A., Tavoni, M., (2016), The Shared Socioeconomic Pathways and their energy, land use, and greenhouse gas emissions implications: An overview, *Global Environmental Change*, **42**, pp. 153-168 , DOI: 10.1016/j.gloenvcha.2016.05.009
25. Sabine, C. L, Feely, R. A, Gruber, N. Key, R. M., Lee, K., Bullister, J. L, Wanninkhof, R., Wong, C. S., Wallace, D. W. R, Tilbrook, B., Millero, F. J, Peng, T., Kozyr, A., Ono, T. and Rois, A. F., (2004), The Oceanic Sink for Anthropogenic CO_2, *Science*, **305(5682)**, pp. 367-371, DOI: 10.1126/science.1097403
26. Siegenthaler, U., Stocker, T.F., Monnin, E., Lüthi, D., Schwander, J., Stauffer, B., Raynaud, D., Barnola, J-M., Fischer, H., Masson-Delmotte, V., and Jouzel, J., (2005), Stable Carbon Cycle-Climate Relationship During the Late Pleistocene, *Science*, **310**, pp. 1313-1317, DOI: 10.1126/science.1120130
27. Siegenthaler, U., Monnin, E., Kawamura, K., Spahni, R., Schwander, J., Stauffer, B., Stocker, T.F., Barnola, J.M., and, Fischer, H., (2017), Supporting evidence from the EPICA Dronning Maud Land ice core for atmospheric CO_2 changes during the past millennium, *Tellus B: Chemical and Physical Meteorology*, **57:1**, pp. 51-57, DOI: 10.3402/tellusb.v57i1.16774,
28. SSP Public Database version 1.1 (2018), https://tntcat.iiasa.ac.at/SspDb
29. Takahashi, T., Sutherland, S. C., Sweeney, C. Poisson, A., Metzl, N., Tilbrook, B., Bates, N., Wanninkhof, R., Feely, R. A., Sabine, C., Olafsson, J., and Nojiri, Y., (2002), Global sea-air CO_2 flux based on climatological surface ocean $p$$CO_2$, and seasonal biological and temperature effects, *Deep Sea Research Part II: Topical Studies in Oceanography,* **49 (9–10)**, pp. 1601-1622, DOI: 10.1016/S0967-0645(02)00003-6
30. van Vuuren, D.P., Stehfest, E., Gernaat, D.E.H.J., Doelman, J.C., van den Berg, M., Harmsen, M., de Boer, H.S., Bouwman, L.F., Daioglou, V., Edelenbosch, O.Y., Girod, B., Kram, T., Lassaletta, L., Lucas, P.L., Meijl, H., Müller, C., van Ruijven, B.J., van der Sluis, S., Tabeau, A., (2016), Energy, land-use and greenhouse gas emissions trajectories under a green growth paradigm, *Global Environmental Change*, (**42**), pp. 237-250, DOI: 10.1016/j.gloenvcha.2016.05.008
31. Wikipedia (2018), https://en.wikipedia.org/wiki/Radiative_forcing#Forcing_due_to_atmospheric_gas